EAST EUROPEAN JOURNAL OF PHYSICS. **1.** 77-84 (2022)
DOI:10.26565/2312-4334-2022-1-11 ISSN 2312-4334

# INTERACTIONS OF NOVEL PHOSPHONIUM DYE WITH LIPID BILAYERS: A MOLECULAR DYNAMICS STUDY†

**Olga Zhytniakivska***
*Department of Medical Physics and Biomedical Nanotechnologies, V.N. Karazin Kharkiv National University*
*4 Svobody Sq., Kharkiv, 61022, Ukraine*
**Corresponding Author: olga.zhytniakivska@karazin.ua*
Received February 1, 2022; revised February11, 2022; accepted February 14, 2022

In the present work the 100-ns molecular dynamics simulations (MD) were performed in the CHARMM36m force field using the GROMACS package to estimate the bilayer location and mechanisms of the interaction between the novel phosphonium dye TDV and the model lipid membranes composed of the phosphatidylcholine (PC) and its mixtures with cholesterol (Chol) or/and anionic phospholipid cardiolipin (CL). Varying the dye initial position relative to the membrane midplane, the dye relative orientation and the charge state of the TDV molecule it was found that the one charge form of TDV, which was initially translated to a distance of 20 Å from the membrane midplane along the bilayer normal, readily penetrates deeper into the membrane interior and remains within the lipid bilayer during the entire simulation time. It was revealed that the probe partitioning into the model membranes was accompanied by the reorientation of TDV molecule from perpendicular to nearly parallel to the membrane surface. The analysis of the MD simulation results showed that the lipid bilayer partitioning and location of the one charge form of TDV depend on the membrane composition. The dye binds more rapidly to the neat PC bilayer than to CL- and Chol-containing model membranes. It was found that in the neat PC and CL-containing membranes the one charge TDV resides at the level of carbonyl groups of lipids (the distances ~ 1.1 nm, 1.2 nm and 1.3 nm from the bilayer center for the PC, CL10 and CL20 lipid membranes, respectively), whereas in the Chol-containing membranes the probe is located at the level of glycerol moiety (~ 1.5 nm and 1.6 nm for the Chol30 and CL10/Chol30 lipid membranes, respectively). It was demonstrated that the dye partitioning into the lipid bilayer does not affect the membrane structural properties.
**Keywords**: Phosphonium dye, lipid bilayer, molecular dynamics simulation.
**PACS:** 87.14.C++c, 87.16.Dg

In recent years, molecular dynamics simulation has emerged as a powerful computation tool for investigating a wide variety of biological systems [1-27]. Specifically, MD simulations have been used i) to characterize the structure of the lipid membranes [1-4], proteins [5-8] or nucleic acids [9-12]; ii) to study the physicochemical properties of the isolated virus proteins or capsids [13-16]; iii) to elucidate the nature of the energy transport in the light-harvesting complexes [17,18]; iv) to ascertain the binding mode of a therapeutic agent to a given biological target in the drug design strategies [19-22]; v) to identify antiviral inhibitors [23-25], to name only a few. Likewise, MD simulation appeared to be especially useful in examining the structural, physicochemical and thermodynamic properties of the ligand-macromolecule systems [26-30]. In particular, MD simulation has provided a unique framework for the atomic-level characterization of interactions between ligands and membranes [30-39]. A good deal of studies indicate that MD simulations can be used to achieve a fundamental understanding of the mechanisms underlying the interaction of proteins [31,32], peptides [33, 34] and drugs [35, 36] with lipid membranes. Notably, MD approaches appeared to be highly efficient in exploring the behavior of fluorescent membrane probes, that is of great importance for their biomedical application and synthesis of new fluorescent reporter molecules with improved properties [37-46]. To exemplify, the molecular dynamics simulation was used to develop a molecular design strategy of AIE-based fluorescent probes for selective targeting of mitochondrial membrane [37]; to characterize the partitioning and membrane disposition of the diphenylhexatriene probes [38], to characterize the solvation behavior of phthalocyanines [39], to explore the dynamical behavior of the DiI carbocyanine derivative in a lipid bilayer [40], to estimate the membrane location of ESIPT fluorophores [41], coumarin derivatives [42], benzanthrone dye [43] and membrane polarity probes Prodan and Laurdan [44,45], to investigate the interactions of methylene blue with oxidized and non-oxidized lipid bilayers [46], to name only a few.

The aim of the present study was to explore the interaction of the novel phosphonium dye TDV (Fig. 1) with the model lipid membranes of different composition using the molecular dynamics simulation. To this end, the 100 ns MD simulations were carried out for TDV with the neat phosphatidylcholine bilayer (PC) and bilayers from PC mixtures with: i) anionic lipid cardiolipin (CL) with the PC:CL molar ratio 9:1 and 4:1 (denoted here as CL10 and CL20, respectively); ii) sterol cholesterol (Chol) with the PC:Chol ratio 7:3 (Chol30); iii) both CL and Chol lipids with the PC:CL:Chol ratio 6:1:3 (CL10/Chol30). To obtain the optimal conditions for the TDV-membrane simulations and an atomistically detailed picture of the TDV binding to the lipid bilayers, the MD calculations were performed at varying initial positions of the dye and its orientation relative to the bilayer normal. Moreover, to estimate the role of electrostatic interactions in the TDV membrane partitioning, two dye forms were considered for the simulation. The

† ***Cite as***: O. Zhytniakivska, East. Eur. J. Phys. **1**, 77 (2022), https://doi.org/10.26565/2312-4334-2022-1-11

first form of the TDV molecule possessed two positive charges (on the P atom of the phosphonium group and the N atom of the pyridine ring), while in the second one the charge on the P atom of the phosphonium group was neutralized by the iodine ion (one charge dye form).

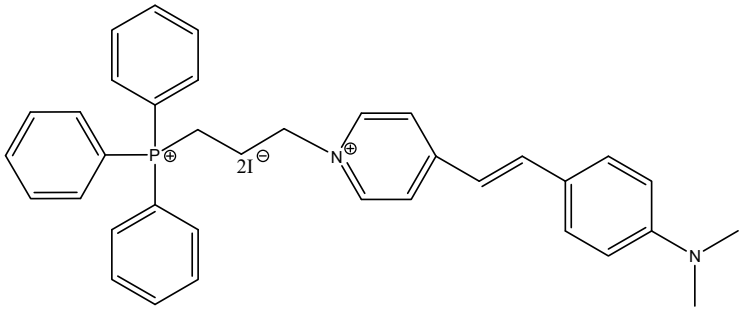


**Figure 1.** The structural formula of TDV

## EXPERIMENTAL SECTION

### System description

The input files of TDV-membrane systems for MD calculations were prepared using the web-based graphical interface CHARMM-GUI [47]. The .pdb-file of TDV was generated in OpenBabelGUI 2.4.1, using the structure drawn in MarvinSketch (mrv format). Two different dye structures were created for MD simulations, with total charges +2 and +1, respectively. In both cases the atomic charges of TDV were corrected using the RESP ESP charge Derive Server. The topology of TDV was generated using the CHARMM-GUI Ligand Reader and Modeler [48]. The obtained files were further used to generate the dye-lipid systems using the Membrane Builder option [49]. MD simulations were carried out for TDV with five different membrane systems with a nearly identical number of lipids. The first one was composed of TDV and 94 1-palmitoyl-2-oleoyl-*sn*-glycero-3-phosphatidylcholine (POPC) molecules in each monolayer. Hereafter, the neat POPC bilayer is referred to as PC. Two systems were represented by TDV and bilayers from POPC mixtures with anionic lipid cardiolipin (LOCCL2 lipid component in the CHARMM-GUI lipid bank) with the POPC:LOCCL2 ratios 9:1 and 4:2, referred to here as CL10 and CL20, respectively. The fourth type of the lipid bilayer (Chol30) was composed from TDV, 77 POPC and 33 cholesterol molecules in each monolayer (POPC:Chol ratio 7:3). The last type of lipid bilayers was composed from PC mixture with both CL and Chol lipids with the POPC:LOCCL2:Chol ratio 6:1:3 (CL10/Chol30). The initial distance of the TDV translation from the membrane midplane along the bilayer normal was varied from 0 to 30 Å. To obtain a neutral total charge of the system a necessary number of counterions was added.

### Molecular dynamics simulation and data analysis

Molecular dynamics simulations and analysis of the trajectories were carried out using the GROMACS software (version 5.1) with the CHARMM36m force field in the NPT ensemble with the time step for MD simulations 2 fs. Calculations were performed at a temperature of 310 K. The Particle Mesh Ewald method was utilized for correct treatment of the long-range electrostatic interactions [50]. The bond lengths were constrained using the LINC algorithm [51]. The pressure and temperature controls were performed using the Berendsen thermostat [52]. MD simulations were performed with minimization of 50000 steps and equilibration of 12500000 steps. The whole time interval for MD calculations was 100 ns. The GROMACS command gmx density was used to calculate the mass density distribution for various components of the lipid bilayer and density distribution of TDV across a lipid bilayer. The analyses of the membrane thickness, membrane area and area per lipid were conducted using the FATSLiM package [53]. The molecular graphics and visualization of the simulation evolution over time were performed using the Visual Molecular Dynamics VMD software.

## RESULTS AND DISCUSSION

TDV, a phosphonium-based water-soluble fluorescent dye, has been reported to have a marked ability to biomolecular interactions. Specifically, it was demonstrated that TDV can be effectively used for optical detection of disease-related protein aggregates [54,55] and for elucidating the mechanisms of DNA interactions with amyloid fibrils [56]. Moreover, it was shown previously that TDV is highly suitable for membrane studies since it possesses a pronounced lipid-associating ability and high sensitivity to physicochemical properties of the model lipid bilayers [57]. In the present study the molecular dynamics simulation was used to explore the interaction between TDV and the model lipid membranes with the main emphasis on determining the depth of the probe location in a lipid bilayer. Besides, it was assumed previously that membrane electrostatics plays an important role in the membrane association of TDV [57]. Therefore, it was also interesting to assess the role of TDV charge in the dye membrane partitioning.

At the first step of study, the MD calculations were performed for the TDV molecule bearing two positive charges (on the P atom of the phosphonium group and on the N atom of the pyridine ring). Specifically, the TDV molecule was

initially translated to a distance of 30 Å from the membrane midplane along the bilayer normal. The phosphonium group of the TDV molecule was directed from the membrane center. In this case the TDV molecule did not show affinity to the PC bilayer during the entire simulation time (Fig.2 B). Probably, the formation of the hydration shell around the water-soluble dye hinders its penetration in the lipid bilayer. Similar behavior was observed for the phthalocyanine dye in the POPC bilayers [39]. The simulation was performed also for the mixed bilayers containing negatively charged cardiolipin and sterol cholesterol, but in both these cases the TDV-lipid binding did not occur (data not shown). Therefore, the MD calculations were carried out at varying the dye initial position from the membrane midplane along the bilayer normal. Moreover, initial location of the dye in the region of lipid headgroups at a distance 20 Å from the membrane center or at the bilayer midplane (Fig. 2 C) didn't change the final result, since to the end of the 100 ns simulation the TDV molecule left the membrane interior (Fig. 2 B,D. The MD simulations were also performed for the systems where the phosphonium group of the TDV molecule was oriented toward the membrane center, but the no TDV-membrane binding was found (data not shown). These MD data are in controversy with the experimental studies [57] providing evidence for strong partitioning of TDV into lipid bilayers of different composition. The most probable reason for the observed inconsistences between the experimental data and modeling is the charge distribution over the dye molecule, rendering the penetration into membrane interior energetically unfavorable. Another possible reason is the short simulation period.

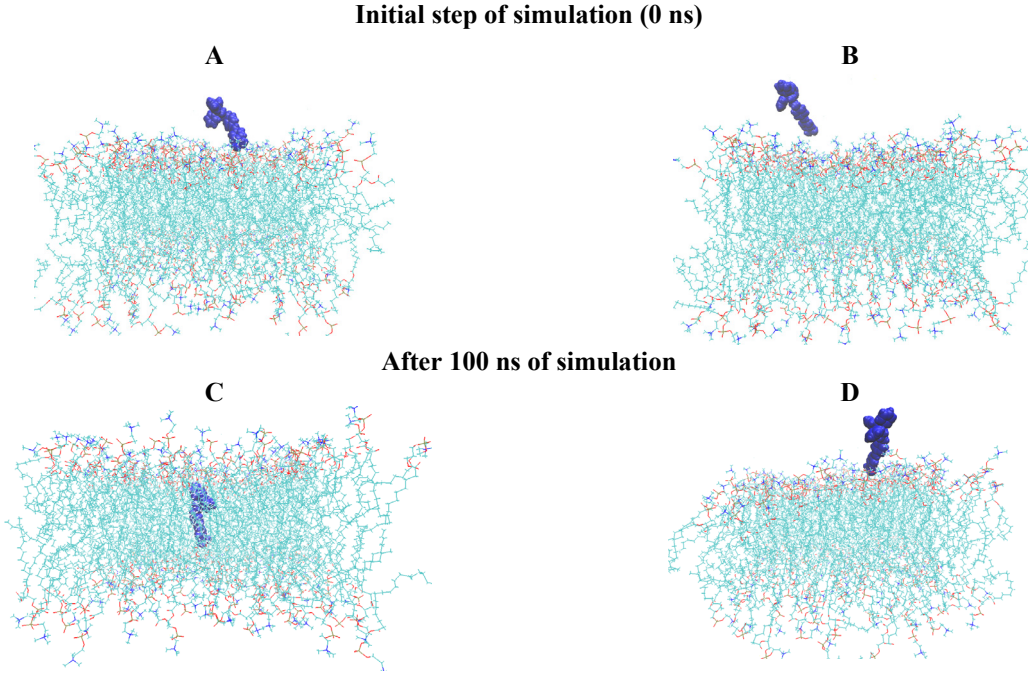


**Figure 2. S**napshots of TDV in the PC lipid bilayer at the initial step (**A, C**) and after 100 ns (**B, D**) of simulation. The TDV molecule was translated perpendicular to the lipid bilayer to a distance of 30 Å (panel A) from the membrane midplane along the bilayer normal. Panel C represents transmembrane location of the TDV (0 Å). The TDV molecule is depicted in blue using the VDW drawing method. The lipid tails are represented as sticks in cyan, the phosphorus and nitrogen atoms of the lipid headgroups are shown by orange and blue, respectively. For clarity, water molecules and ions are not shown

The numerous studies indicate that the charge of fluorescent dye exerts significant influence on the probe affinity to the lipid membranes and its bilayer location [37, 40, 46]. Specifically, it was shown previously that the cationic and neutral forms of methylene blue display different affinities to the oxidized and non-oxidized lipid bilayers [46]. Specifically, the comparison of the results of molecular dynamics modelling of methylene blue interaction with the control and peroxidized DOPC lipid bilayers for the cationic dye form, neutral MB (reduced dye form) and neutral MB in the form of the undissociated salt indicates the stronger dye-lipid interaction of the cationic MB with the peroxidized lipids [46]. Moreover, the cationic MB exerts significant impact on the membrane area and the later diffusion of the peroxidized lipid bilayer [46]. The charge on the dye headgroups was shown to play a significant role in the bilayer translocation of the AIEgen fluorescent dyes [37]. Moreover, the MD simulation of the uncharged and charged carbocyanine dyes revealed the effect of headgroup charge on the dye orientation and bilayer location [40]. Therefore, at the next step of study it was interesting to ascertain how the charge on phosphonium head of the TDV molecule affects the dye- membrane partitioning. To this end, the 100 ns MD simulations were carried out for the TDV cationic form (the charge on the P atom of the phosphonium group was neutralized by the iodine ion) with the neat phosphatidylcholine bilayer and PC mixtures with cholesterol or/and anionic phospholipid cardiolipin. Fig. 3 illustrates the disposition of the one charge form of TDV with respect to lipid/water interface at different simulation times for the PC, CL10 and CL20 lipid bilayers.

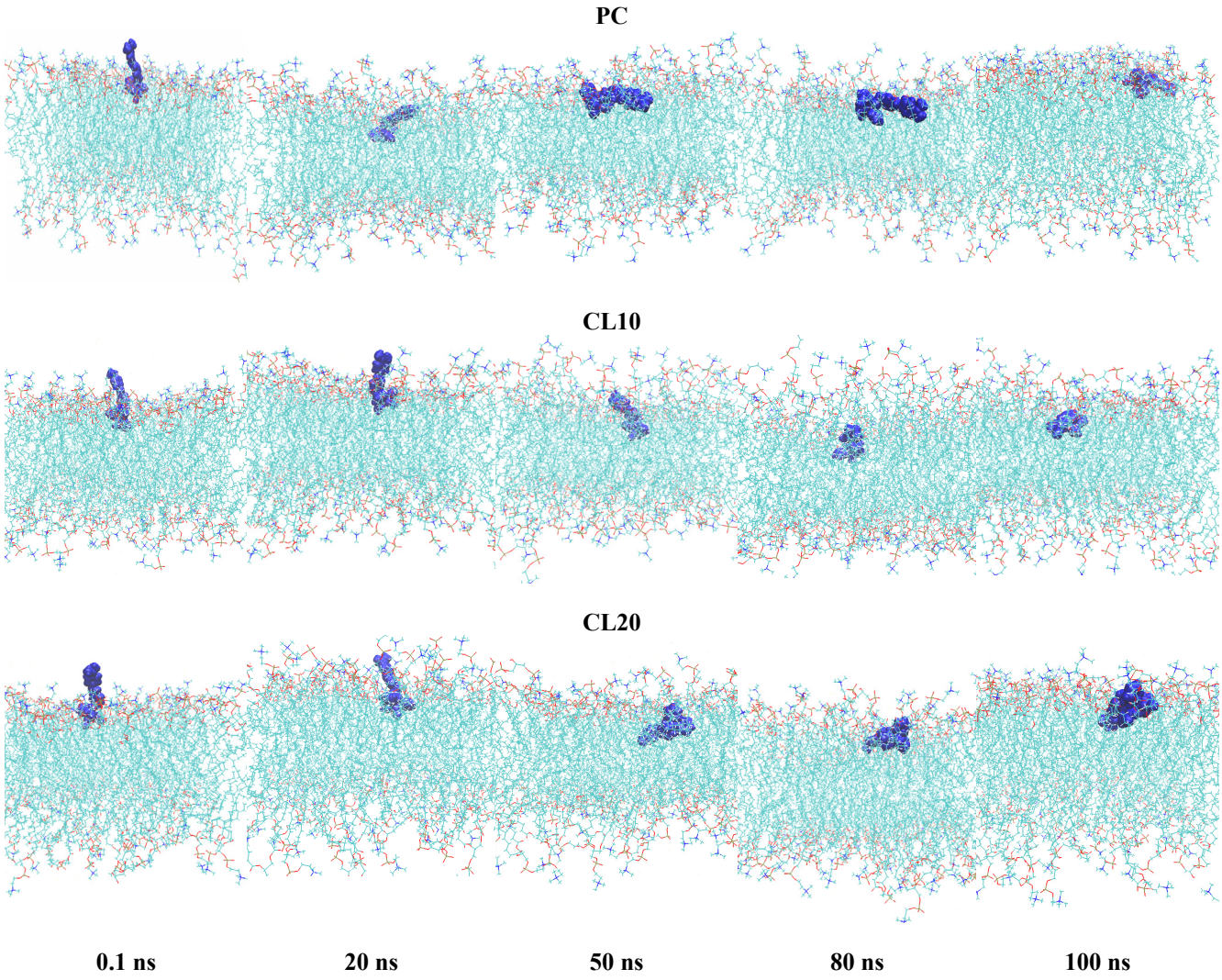


**Figure 3.** The snapshots of the partitioning of the one charge TDV into PC, CL10 and CL20 bilayers at different simulation time points. The TDV molecule is depicted in blue using the VDW drawing method. The lipid tails are represented as sticks in cyan, the phosphorus and nitrogen atoms of the lipid headgroups are shown by orange and blue, respectively. For clarity, water molecules and ions are not shown.

As can be seen from a simple visual inspection of simulation snapshots, the dye molecule which was initially translated to a distance of 20 Å from the membrane midplane along the bilayer normal moved deeper to the membrane interior and remained within the lipid bilayer for the rest of simulation time. The cationic form of TDV appeared to be sensitive to the changes in physicochemical properties of the lipid bilayers. More specifically, MD simulation demonstrated that the probe binds more rapidly to the neat PC bilayers than to CL-containing model membranes, penetrating deeper into bilayer interior after ~ 20 ns of simulation. Meanwhile, after 20 ns of MD calculation, the phosphonium group of the one chargeTDV is positioned in the hydrophobic tail region, while the positively charged pyridine ring is localized at the level of the carbonyl groups of the polar/nonpolar interface. The partitioning of the one charge TDV into CL-containing membranes was accompanied only by a slight probe reorientation during the first 20 ns of simulations. Thereafter, the dye orientation changed from the perpendicular to the parallel (PC, CL10) or nearly parallel (CL20) to the membrane surface. The above effect was followed by the deeper penetration of the one charge TDV to the CL-containing lipid membranes, while in the neat PC bilayer the dye molecule became less buried due to the phosphonium group relocation to the same level as the rest of the molecule.

Fig.4 shows the snapshots of the partitioning of the one charge TDV into the Chol30 and CL10/Chol30 bilayers. During the first 20 ns of the simulations the reorientation of the probe was observed coupled with a slight penetration of the dye molecule to the membrane interior. Likewise, during the following period of time the position of the dye phosphoniun head remained virtually unchanged while the positively charged tail tended to reside in the proximity to glycerol moiety of the lipid bilayers. Interestingly, the analysis of the positions occupied by the one charge TDV over the MD trajectory in the case of neat PC, CL or Chol containing membranes indicates that this probe prefers the orientation parallel to the membrane surface. Moreover, in the presence of cholesterol TDV tends to occupy more polar membrane binding sites. Fig.5 shows the time evolution of the separation between the dye center of mass and the bilayer center.

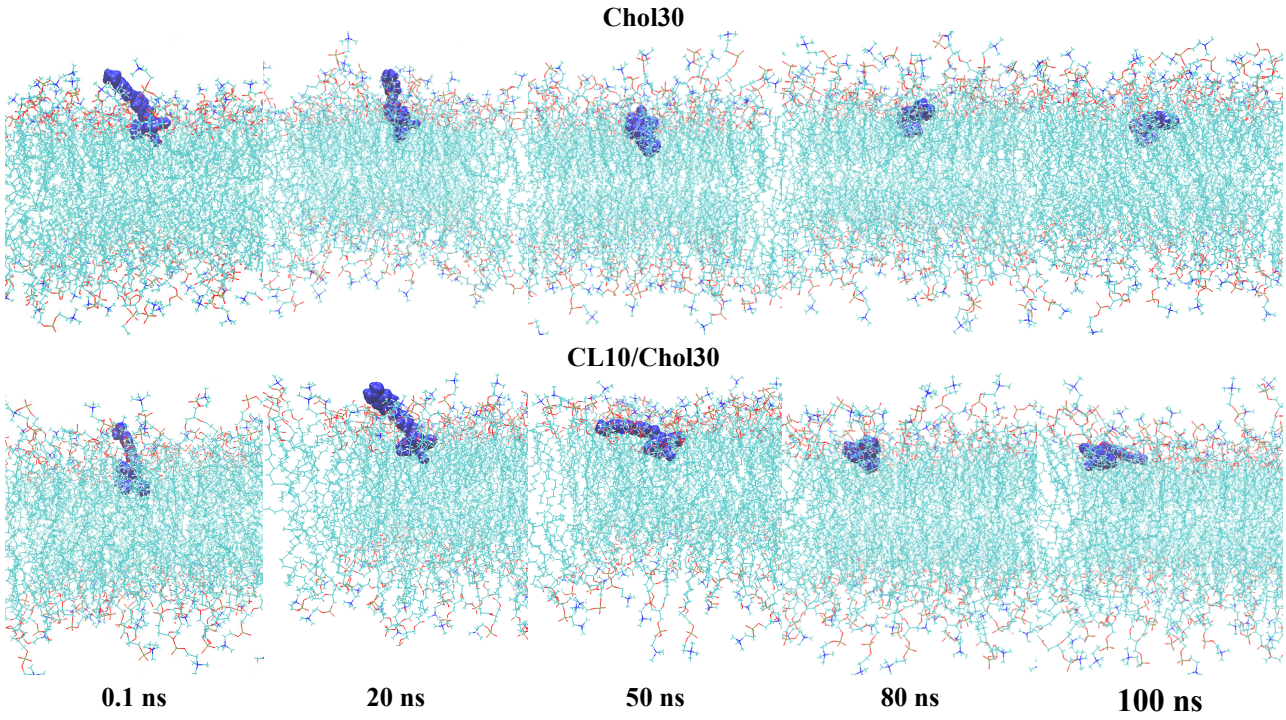


**Figure 4.** The snapshots of the partitioning of the one charge TDV into Chol30 and CL10/Chol30 bilayers at different simulation time points. The TDV molecule is depicted in blue using the VDW drawing method. The lipid tails are represented as sticks in cyan, the phosphorus and nitrogen atoms of the lipid headgroups are shown by orange and blue, respectively. For clarity, water molecules and ions are not shown.

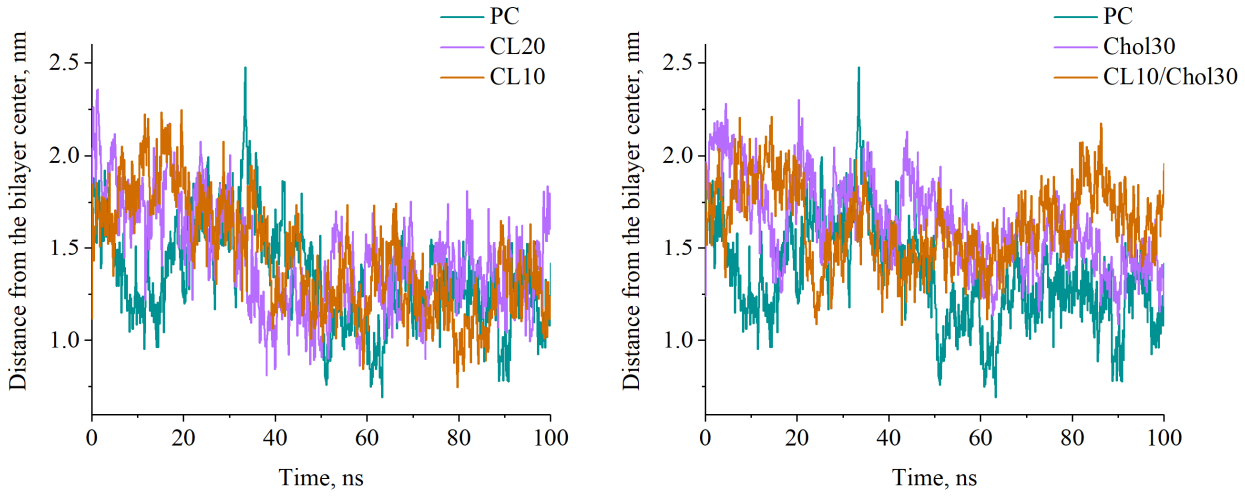


**Figure 5.** Time evolution of the TDV distance from the bilayer center

In order to determine the precise TDV location, the mass density distribution profiles of the dye, water and the molecular groups of lipids were plotted with respect to the bilayer normal (Fig. 6). As can be seen, the peak of the one charge TDV mass distribution in the PC (Fig. 6A), CL10 (Fig. 6B) and CL20 (Fig.6 C) bilayers is observed at the distances ~ 1.1 nm, 1.2 nm and 1.3 nm from the bilayer center. According to the partial density profile of the lipid membrane proposed by Marrink and Berendsen [58], a lipid bilayer can be divided into four regions: 1) the region of the hydrophobic lipid tails (0-8 Å from the membrane center); 2) the interfacial region between the upper carbons of hydrophobic tails and hydrophilic headgroups (8-16 Å from the membrane center); 3) the interfacial area containing negatively charged phosphate groups, positively charged choline groups and (16-25 Å) from the membrane center); 4) the region of the bulk water (>25 Å).

Therefore, in the PC and CL-containing membranes TDV resides in the region of carbonyl groups. In the Chol30 (Fig. 6 D) and CL10/Chol20 (Fig. 6 E) lipid membranes the peak of the dye distribution is observed at 1.5 nm and 1.6 nm, respectively, assuming the probe location at the level of glycerol moiety.

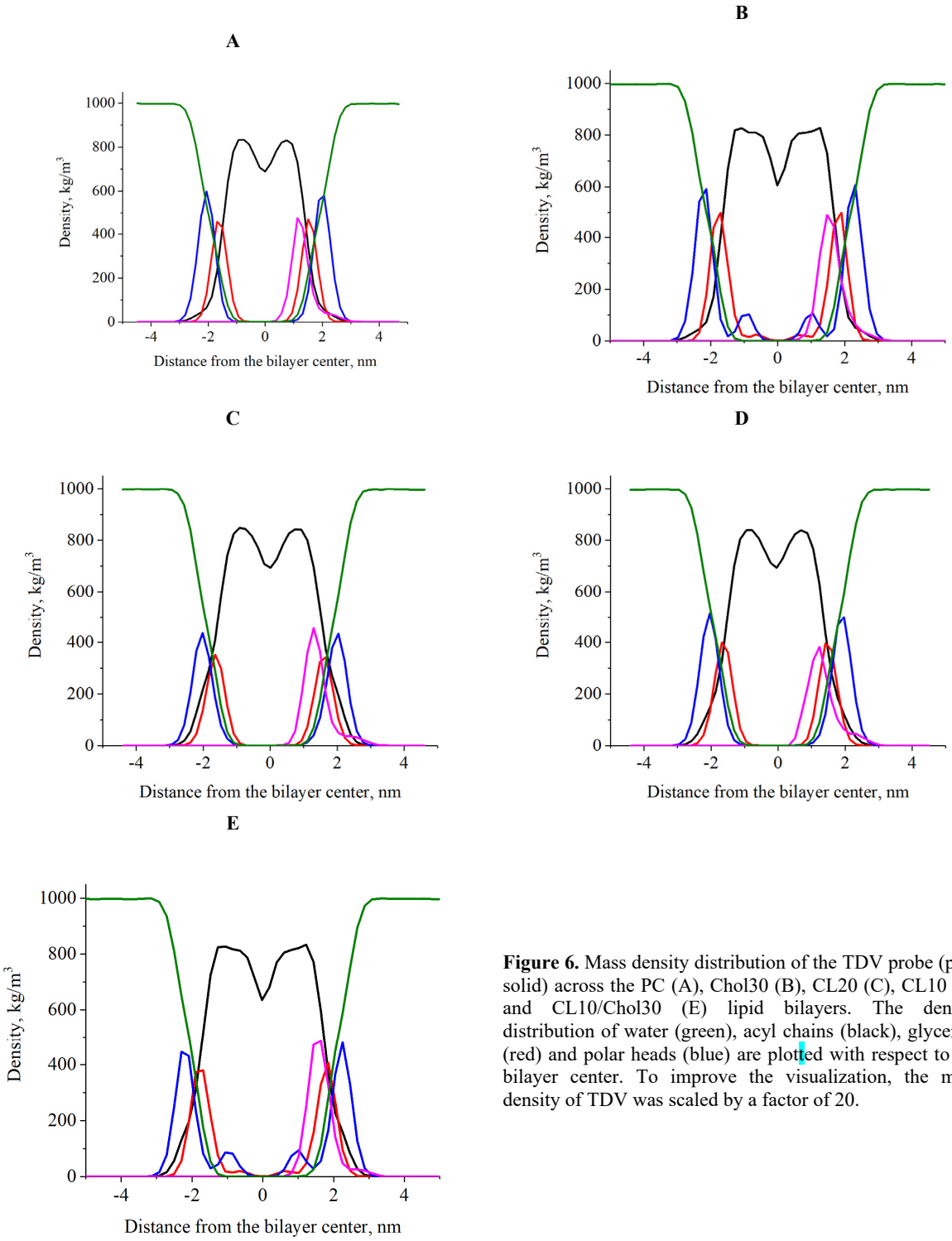


**Figure 6.** Mass density distribution of the TDV probe (pink solid) across the PC (A), Chol30 (B), CL20 (C), CL10 (D) and CL10/Chol30 (E) lipid bilayers. The density distribution of water (green), acyl chains (black), glycerols (red) and polar heads (blue) are plotted with respect to the bilayer center. To improve the visualization, the mass density of TDV was scaled by a factor of 20.

**Table 1**. Average properties of lipid bilayers in the presence of the one charge TDV

| | Control bilayers | | In the presence of the dye | |
|---|---|---|---|---|
| System | Membrane thickness (nm) | Area per lipid head group ($nm^2$) | Membrane thickness (nm) | Area per lipid head group ($nm^2$) |
| PC | 3.886±0.06 | 0.656±0.012 | 3.895±0.058 | 0.652±0.012 |
| CL10 | 4.438±0.056 | 0.695±0.012 | 4.448±0.072 | 0.689±0.014 |
| CL20 | 3.951±0.066 | 0.971±0.022 | 3.946±0.065 | 0.967±0.022 |
| Chol30 | 3.960±0.059 | 0.785±0.013 | 3.903±0.056 | 0.792±0.013 |
| CL10/Chol30 | 4.370±0.062 | 0.938±0.027 | 4.345±0.057 | 0.929±0.022 |

To investigate the influence of the TDV one charge form on the structural properties of lipid bilayers, the average area per lipid head group and the membrane thickness were calculated for the dye-free PC, CL10, CL20, Chol30 and CL10/Chol30 bilayers and for the systems with one charge TDV. As seen in Table 1, the TDV does not significantly perturb the lipid bilayer structure.

## CONCLUSIONS

To summarize, in the present study a 100 ns molecular dynamics simulation was performed to explore the interaction of the novel phosphonium dye TDV with the model lipid membranes composed of phosphatidylcholine and its mixtures with cholesterol or/and anionic phospholipid cardiolipin with the main emphasis on the determination of the probe bilayer location. It was found that the one charge form of TDV, which was initially translated to a distance of 20 Å from the membrane midplane along the bilayer normal, readily incorporates deeper into the membrane interior and remains within the lipid bilayer during the entire simulation time. The probe partitioning into the model membranes was accompanied by the TDV molecule reorientation from perpendicular to nearly parallel to the membrane surface. It was shown that the charge on the phosphonium group of the TDV molecule plays a significant role in the dye membrane partitioning.

## ACKNOWLEDGEMENTS

This work was supported by the Ministry of Education and Science of Ukraine (the Young Scientist projects № 0120U101064 "Novel nanomaterials based on the lyophilic self-assembled systems: theoretical prediction, experimental investigation and biomedical applications" and the project No. 0119U002525 "Development of novel ultrasonic and fluorescence techniques for medical micro- and macrodiagnostics"). The author is grateful to Prof. Galyna Gorbenko and Dr. Uliana Tarabara, V.N. Karazin Kharkiv National University, for useful comments and discussions.

## ORCID IDs

**Olga Zhytniakivska,** https://orcid.org/0000-0002-2068-5823

## REFERENCES

[1] R.M. Venable, A. Kramer, R.W. Pastor, Chem. Rew. **119**, 5954-5997 (2019). https://doi.org/10.1021/acs.chemrev.8b00486.
[2] M.L. Berkowitz, Biochim. Biophys. Acta. **1788**, 86-96 (2009). https://doi.org/10.1016/j.bbamem.2008.09.009
[3] M. Pasenkiewicz-Gierula, T. Rog, K. Kitamura, A. Kusumi, Biophys J. **78**, 1376-1389 (2000), https://doi.org/10.1016/S0006-3495(01)75867-5.
[4] T. Rog, M. Pasenkiewicz-Gierula, FEBS Letters, **502**, 68-71 (2000). https://doi.org/10.1016/S0014-5793(01)02668-0.
[5] L. Heo, M. Feig, PNAS, **115**, 13276-13281 (2018). https://doi.org/10.1073/pnas.1811364115.
[6] B. Urbanc, M. Betnel, L. Cruz, G. Bitan, D.B. Teplow, J. Am. Chem. Soc., **132**, 4266-4280 (2010). https://doi.org/10.1021/ja9096303.
[7] Z. Qin, M. J. Buehler, Phys. Rev. Lett. **104**, 198304 (2010). https://doi.org/10.1103/PhysRevLett.104.198304.
[8] L. Tran, T. Ha-Duong, Peptides, **69**, 86-91 (2015). https://doi.org/10.1016/j.peptides.2015.04.009.
[9] A. D. MacKerell, N. K. Banavali, J. Comp. Chem. **21**, 105-120 (2000). https://doi.org/10.1002/(SICI)1096-987X(20000130)21:2<105::AID-JCC3>3.0.CO;2-P.
[10] K.E. Furse, S. A. Corcelli, J. Phys. Chem. Lett. **1**, 1813-1820 (2010). https://doi.org/10.1021/jz100485e.
[11] A. Noy, A. Perez, F. Lankas, F.J. Luque, M. Orozco. J. Mol. Biol. **343**, 627-638 (2004). https://doi.org/10.1016/j.jmb.2004.07.048.
[12] I.-C. Yeh, G. Hummer. Biophys. J. **86**, 681-689 (2004). https://doi.org/10.1016/S0006-3495(04)74147-8.
[13] H. Ode, M. Nakashima, S. Kitamura, W. Sugiura, H. Sato, Front. Microbiol. **3**, 00258 (2012). https://doi.org/10.3389/fmicb.2012.00258.
[14] J.R. Perilla, J.A. Hadden, B.C. Goh, C.G. Mayne, K. Schulten, J. Phys. Chem. Lett. **7**, 1836-1844 (2016). https://doi.org/10.1021/acs.jpclett.6b00517.
[15] D. Suarez, N. Diaz, J. Chem. Inf. Model. **60**, 5815-5831 (2020). https://doi.org/10.1021/acs.jcim.0c00575.
[16] C. M. Quinn, M. Wang, M. P. Fritz, B. Runge, J. Ahn, C. Xu, J.R. Perilla, A. Grohenborn, T. Polenova, PNAS, **115**, 11519-11524 (2018). https://doi.org/10.1073/pnas.1800796115.
[17] A. Damjanović, I. Kosztin, U. Kleinekathöfer, K. Schulten. Phys. Rev. E. **65**, 031919 (2002). https://doi.org/10.1103/PhysRevE.65.031919.
[18] D. Chandler, J. Strumpfer, M. Sener, S. Scheuring, K. Schulten, Biophys. J. **106**, 2503-2510 (2014). https://doi.org/10.1016/j.bpj.2014.04.030.
[19] L. Liang, J.-W. Shen, Q. Wang, Colloids Surf. B **153**, 168-173 (2017). https://doi.org/10.1016/j.colsurfb.2017.02.021.
[20] H. Zhao, A. Caflisch, Eur. J. Med. Chem. **91** 4-14 (2015). https://doi.org/10.1016/j.ejmech.2014.08.004.
[21] P.-C. Do, E.H. Lee, L. Le, J. Chem. Inf. Model. **58** 1473-1482 (2018). https://doi.org/10.1021/acs.jcim.8b00261.
[22] M. Hernandez-Rodriguez, M. C. Rosales-Hernandez, J. E. Mendieta-Wejebe, M. Martinez-Archundia, J. Correa Basurto, Curr. Med. Chem. **23** 3909-3924 (2016).
[23] J. Wang, C. Ma, G. Fiorin, V. Carnevale, T. Wang, F. Hu, R. Lamb, et al. J. Am. Chem. Soc. **133**, 12834-12841 (2011). https://doi.org/10.1021/ja204969m.
[24] J. Fantini, H. Chahinian, N. Yahi, Int. J. Antimicrob Agents **56**, 106020 (2020). https://doi.org/10.1016/j.ijantimicag.2020.106020.
[25] M. Métifiot, K. Maddali, B. Johnson, S. Hare, S. Smith et al. ACS Chem. Biol. **8**, 209-217 (2012). https://doi.org/10.1021/cb300471n.
[26] Z. Dolenc, C. Oostenbrink, J. Koller, W. van Gusteren, Nucleic Acids Res. **33**, 725-733 (2005). https://doi.org/10.1093/nar/gki195.
[27] T.A. de Oliveira, L.R. Medaglia, E.H. Bechelane Maia, et al. Pharmaceuticals **15**, 132 (2022). https://doi.org/10.3390/ph15020132.
[28] A. Hospital, J.R. Goni, M. Orozco, J. L. Gelpi, Adv. Appl. Bioinform. Chem. **8**, 37-47 (2015). https://doi.org/10.2147/AABC.S70333.

[29] N. Ahalawat, R.K. Murarka, J. Biomol.Struct. Dyn. **33,** 1-13 (2015). https://doi.org/10.1080/07391102.2014.996609.
[30] Y. Fu, J. Zhao, Z. Chen, Comput. Math. Methods Med. **2018,** 3502514 (2018). https://doi.org/10.1155/2018/3502514.
[31] K. Goossens, H. De Winter, J. Chem. Inf. Model. **58,** 2193-2202 (2018). https://doi.org/10.1021/acs.jcim.8b00639.
[32] J. Loschwitz, O. Olubiyini, J.S. Hub, B. Strodel, H.S. Poojari, PMBTS, **170,** 273-403 (2020). https://doi.org/10.1016/bs.pmbts.2020.01.001.
[33] Yi. Wang, D.E. Schalamadinger, J.D. Kim, J.A. McCammon, Biochim. Biophys. Acta, **1818**, 1402-1409 (2012). https://doi.org/10.1016/j.bbamem.2012.02.017.
[34] H. Jang, B. Ma, T.Woolf, R. Nussinov, Biophys. J., **91**, 2848-2859 (2006). https://doi.org/10.1529/biophysj.106.084046.
[35] T.J, Yacoub, A.S. Reddy, I. Szleifer, Biophys J. **101**, 378-385 (2011). https://doi.org/10.1016/j.bpj.2011.06.015.
[36] A. Kabedev, S. Hossain, M. Hubert, P. Larson, C. Bergstrom, J. Pharm. Sci. **110**, 176-185 (2021). https://doi.org/10.1016/j.xphs.2020.10.061.
[37] X. Zheng, D. Wang, W. Xu, S. Cao, Q. Peng, B. Zhong Tang, Mater. Horiz. **6**, 2016-2023 (2019). https://doi.org/10.1039/C9MH00906J.
[38] A.M.T.M. do Canto, J.R. Robalo, P.D. Santos, et al., Biochim. Biophys. Acta, **1858**, 2647-2661 (2016), https://doi.org/10.1016/j.bbamem.2016.07.013.
[39] P. S. Orekhov, E. G. Kholina, M. E. Bozdaganyan, A. M. Nesterenko, I.B. Kovalenko, M. G. Strahovskaya, J. Phys. Chem. B **122**, 3711-3722 (2018). https://doi.org/10.1021/acs.jpcb.7b11707.
[40] R.P. Gullapalli, M. Demirel, P.J. Butler, Phys Chem Chem.Phys. **10**, 3548-3560 (2008). https://doi.org/10.1039/b716979e.
[41] Y.O. Posokhov, A. Kyrychenko, Biophys. Chem. **235**, 9-18 (2018). https://doi.org/10.1016/j.bpc.2018.01.005.
[42] O. Garcia-Beltran, N. Mena, O. Yanez, J. Caballero, V. Vargas, M. Tunes, et al., Eur. J. Med. Chem. **67**, 60-63 (2013), https://doi.org/10.1016/j.ejmech.2013.06.022.
[43] O. Zhytniakivska, East Europian Journal of Physics, **3**, 134-140 (2020). https://doi.org/10.26565/2312-4334-2020-3-17.
[44] M.W. Baig, M. Pederzoli, P. Jurkiewicz, L. Cwiklik, J. Pittner, Molecules, **23**, 1707 (2018). https://doi.org/10.3390/molecules23071707.
[45] J. Barucha-Kraszewska, S. Kraszewski, P. Jurkiewicz, C. Ramseyer, M. Hof, Biochim. Biophys. Acta, **1798**, 1724-1734 (2010). https://doi.org/10.1016/j.bbamem.2010.05.020.
[46] N. I. Ercan, P. Stroeve, J.W. Tringe, R. Faller, Langmuir **34**, 4314-4323 (2018). https://doi.org/10.1021/acs.langmuir.8b00372.
[47] S. Jo, T. Kim, V. G. Iyer, W. Im. J. Comp. Chem. **29**, 1859-1865 (2008). https://doi.org/10.1002/jcc.20945
[48] .S. Kim, J. Lee, S. Jo, C.L. Brooks, H.S. Lee, W. Im, J. Comp. Chem. **38**, 1879-1886 (2017). https://doi.org/10.1002/jcc.24829.
[49] J. Lee, D.S. Patel, J. Ståhle, S-J. Park, N.R. Kern, S. Kim, et al., J. Chem. Theory Comp. **15**, 775-786 (2017), https://doi.org/10.1021/acs.jctc.8b01066.
[50] T. Darden, D. Yolk, L. Pedersen, J. Chem. Phys. **98**, 10089-10092 (1993). https://doi.org/10.1063/1.464397.
[51] B. Hess, H. Bekker, H.J.C. Berendsen, J.G.E.M. Fraaije, J. Comp. Chem. **18**, 1463-1472 (1997). https://doi.org/10.1002/(SICI)1096-987X(199709)18:12<1463::AID-JCC4>3.0.CO;2-H.
[52] H. Berendsen, J. Postma, W. van Gunsteren, A. DINola, J. Haak, J.Chem. Phys. **81**, 3684-3690 (1984). https://doi.org/10.1063/1.448118.
[53] S. Buchoux, FATSLiM/fatslim: FATSLiM v 0.2.1 (2016). http://doi.org/10.5281/zenodo.158942.
[54] G. Gorbenko, V. Trusova, T. Deligeorgiev, N. Gadjev, C. Mizuguchi, H. Saito, J. Mol. Liq. **294** 111675 (2019). https://doi.org/10.1016/j.molliq.2019.111675.
[55] G. Gorbenko, O. Zhytniakivska, K.Vus, U. Tarabara, V. Trusova, Phys. Chem. Chem. Phys. **23**, 14746-14754 (2021). https://doi.org/10.1039/D1CP01359A.
[56] O. Zhytniakivska, U. Tarabara, K.Vus, V. Trusova G. Gorbenko, East. Eur. J. Phys. **2**, 19-26 (2019). https://doi.org/10.26565/2312-4334-2019-2-03.
[57] O. Zhytniakivska, East Europian Journal of Physics, **4**, 107-113 (2021). https://doi.org/10.26565/2312-4334-2021-4-12
[58] S.J. Marrink, H.J.C. Berendsen, J. Phys. Chem. **98**, 4155-4168 (1994). https://doi.org/10.1021/j100066a040.

## ВЗАЄМОДІЯ НОВОГО ФОСФОНІЄВОГО ЗОНДУ З ЛІПІДНИМИ МЕМБРАНАМИ: МОЛЕКУЛЯРНО-ДИНАМІЧНЕ ДОСЛІДЖЕННЯ

**О. Житняківська**

*Кафедра медичної фізики та біомедичних нанотехнологій, Харківський національний університет імені В.Н. Каразіна м. Свободи 4, Харків, 61022, Україна*

У даній роботі з використанням 100-нс молекулярно-динамічного моделювання (MD) у силовому полі CHARMM36m пакету GROMACS досліджено локалізацію в ліпідному бішарі та механізми взаємодії між новим фосфонієвим барвником TDV та модельними ліпідними мембранами, що складались із фосфатидилхоліну. (ФС) та його сумішей з холестерином (Холl) та/або аніонним фосфоліпідом кардіоліпіном (КЛ). При варіюванні початкового положення та орієнтації барвника було виявлено, що однозарядна форма TDV, яка спочатку була розташована на відстані 20 Å від центру бішару, проникає глибше у внутрішню частину мембрани і залишається всередині ліпідного бішару протягом усього часу моделювання. Виявлено, що вбудовування зонду в модельні мембрани супроводжується переорієнтацією молекули TDV з перпендикулярної на паралельну до поверхні мембрани. Результати молекулярно-динамічного дослідження свідчать про те, що розподіл в ліпідну фазу та локалізація однозарядної форми TDV в ліпідному бішарі в значній мірі залежать від складу мембрани. Барвник швидше зв'язується з ФХ-бішаром, у порівнянні з модельними мембранами, що містять КЛ та Хол. Продемонстровано, що у ФХ бішарі та мембранах, що містять КЛ, однозарядна форма TDV локалізується на рівні карбонільних груп ліпідів (на відстані ~ 1.1 нм, 1.2 нм і 1.3 нм від центру бішару для ФХ, КЛ10 і КЛ20 ліпідних мембран, відповідно), тоді як у бішарах, що містили Хол, зонд розташовується на рівні гліцеринів (~ 1,5 нм та 1,6 нм для Хол30 та КЛ10/Хол30 ліпідних мембран, відповідно). Виявлено, що взаємодія барвника з ліпідним бішаром не впливає на структурні властивості мембрани.

**Ключові слова:** фосфонієвий барвник, ліпідний бішар, молекулярно-динамічне моделювання.